LUPINE PUBLISHERS

Drug Designing & Intellectual Properties International Journal

DOI: 10.32474/DDIPIJ.2024.04.000185

ISSN: 2637-4706

Research Article

The Interaction Between Ceramide and The Start Domain of Deleted in Liver Cancer 2 (Dlc2) Provides Hints for Drug Development

Wanpeng Sun[1,2,9,10,11*], Fred Xu[2,4,8], Jinjia Yao[3], Heather Leslie[1,2], Dustin Lippert[2,5,6,7] and Michael R.A. Mowat[1,2,9,11]

[1]*Manitoba Institute of Cell Biology, CancerCare Manitoba*

[2]*Department of Biochemistry and Medical Genetics, University of Manitoba*

[3]*Lecturer Union, Yantai University*

[4]*Departments of Pharmacology and Therapeutics, University of Manitoba*

[5]*Departments of Immunology, University of Manitoba*

[6]*Departments of Internal Medicine, University of Manitoba*

[7]*Manitoba Centre for Proteomics and Systems Biology*

[8]*Manitoba Institute of Child Health, 715 McDermot Avenue, Winnipeg, MB R3E 3P4, Canada*

[9]*Research Institute in Oncology and Hematology, Winnipeg, MB R3E 0V9, Canada*

[10]*The Genomic Centre for Cancer Research and Diagnosis (GCCRD), CancerCare Manitoba*

[11]*Department of Physiology, University of Manitoba*

***Corresponding author:** Wanpeng Sun, Department of Biochemistry and Medical Genetics, University of Manitoba, Canada

Received: May 15, 2024 **Published:** May 22, 2024

Abstract

The genes for Deleted in Liver Cancer (Dlc) are frequently silenced in many cancers. There are three types of Dlc genes. Among them, Dlc1 and Dlc2 genes are tumor suppressor genes, which express the Dlc1 and Dlc2 tumor suppressors. Dlc2 is downregulated in breast, liver, glioblastoma and lung tumors.

In this research, we demonstrated that ceramide can directly bind to the START domain of Dlc2 and subsequentially regulate Dlc2 RhoGAP activity, which contributes to the anti-cancer action of Dlc2 by inactivating the tumorigenic Rho signaling. Indeed, this is the first report that studied the lipid interactions of the START domain on Dlc2. By studying the interactions, we found valuable hints for the development of the personalized precision medicine. We proposed a specific therapy combining both macromolecular drug design and small molecular drug design to effectively treat cancer patients with Dlc2 deficiency. This designed therapy is expected to be highly specific with minimal negative effects.

Keywords: Small Molecular Drug Design; Personalized Medicine; Precision Medicine; Macromolecular Drug Design; Tumor Suppressor; Sun Strategy in Drug Development; Fluorescence Resonance Energy Transfer; Lipid Interaction; Computational Modelling

Introduction

The genes for Deleted in Liver Cancer (Dlc) are frequently silenced in many cancer cases. Dlc deletion is associated with ~ 50% of breast, liver and lung tumors and in over 70% of colon cancers [1]. There are several types of Dlc genes. Among them, Dlc1 and Dlc2 genes are tumor suppressor genes [2], which express the Dlc1 and Dlc2 tumor suppressors, which is a large group of molecules that are capable of controlling cell division [3]. Dlc2 is downregulated in breast, liver, glioblastoma and lung tumors [4].

Same as other Dlc gene products, the Dlc2 has the Rho GTPase-activating (RhoGAP) domain, a STAR-related lipid-transfer (START) domain and sterile alpha motif (SAM) domain. It is noteworthy that Dlc2 is also called STARD13, based on the classification of proteins containing a lipid-transfer START domain. Furthermore, there are different types of START domains. The START domain in Dlc is called START 11 (ceramide transfer protein; CERT). Hereby, we use Dlc2, instead of STARD13, to reduce the confusion. Dlc2 tumor suppressor contains the domain of RhoGAP. The RhoGAP domain inactivates the Rho (Ras homology) [5], which causes the oncogenic transformation and cancer progression [6], via promoting cell motility, tumor transformation and metastasis while inhibiting apoptosis [7][8][9]. Thus, the RhoGAP in Dlc2 acts like a brake, stopping the transforming of a normal cell to a cancer cell. To date, there is no studies that have been performed to discover any enhancers that could enhance the brake: enhancing the Dlc2 RhoGAP action of inhibiting Rho signalling. Comparing with Dlc1, which has been studied in the majority of literature, Dlc2 has been less studies and the details of its anticancer pathway need to be revealed.

To date, it is still unclear how ceramide can interact Dlc2 and, subsequently, alter the Rho activity. The START domain of Dlc proteins belong to the START 11 (ceramide transfer protein; CERT), which is known to bind with ceramide. Interestingly, the same lipid binding pocket is also good to dock sphingosine-1-phosphate, a derivative of ceramide according to our in silico simulation (Figure 1). We speculate that the lipid ceramide and its derivatives (Figure 2) may directly interact with Dlc2 through its START domain [10].

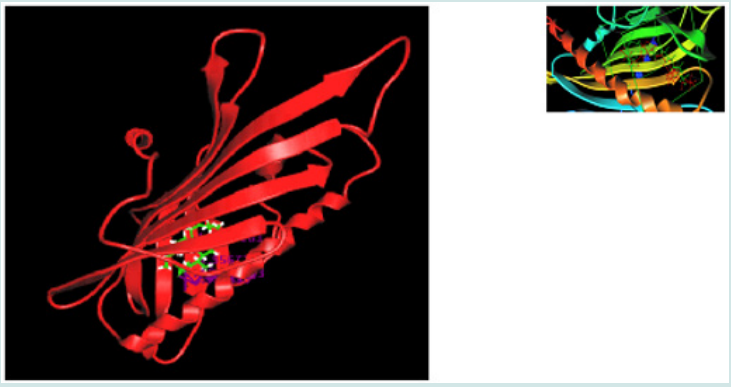

Figure 1: 3D lipid interaction of the CERT START. The START is showed in ribbon structure and acquired from the Protein Data Bank (PDB; # 2E3N). The lipid molecules are shown in the stick model. The same binding pocket for ceramide is also able to dock one of its derivatives. Insect: Both co-crystallization and in silico modelling defined the same ceramide binding pocket of CERT START domain. The green shows the real position of ceramide as determined by co-crystallization [11] and the red shows the in silico simulated position as determined by in silico docking.

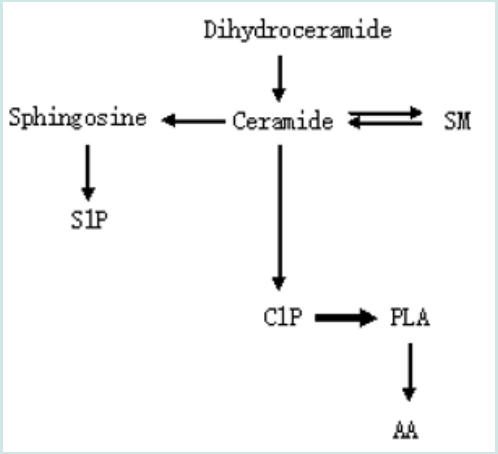

Figure 2: Ceramide and its related lipids. The precursor dihydroceramide (physiologically inactive) is converted to ceramide (physiologically active). Ceramide can be further converted to sphingosine and sphingosine-1-phosphate (S1P) or ceramide-1-phosphate (C1P) or SM (sphingomyelin) which can be hydrolyzed back to ceramide. C1P can interact with phospholipase A (PLA) to produce arachidonic acid (AA).

Our previous research demonstrated that Dlc2 knock-down cells showed a deficiency in ceramide signalling as well as the lack of drug response. The ceramide is not only a lipid, but also an important intermediate molecule in cellular signalling. Many cancer drugs trigger the increase of the amount of the cellular ceramide. Thus, it is speculated that the Dlc2 deficiency causes the deficiency of ceramide signaling, which contributes to the lack of drug response. We hypothesize that the lipid ceramide or its derivatives (Figure 2) may directly interact with Dlc2 through its START domain [10]. Our results support the hypothesis. This study shows that ceramide can directly bind the STAR domain of Dlc2 and alter its RhoGap activity both in vitro and in vivo to suppress Rho activity. Based on the interaction mechanisms, we are designing new therapeutic molecules to precisely treat patients with Dcl2 deficiency.

Results

Cloning, Expression and Purification START Domain

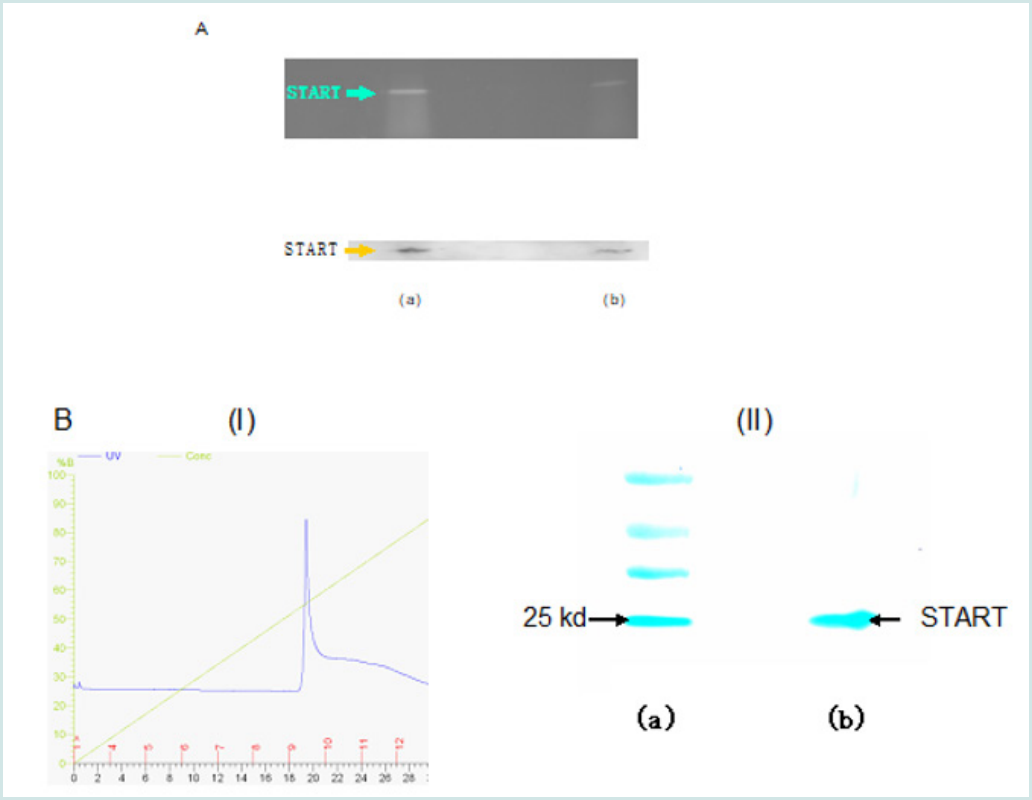

Figure 3: The START domain of Dlc2 was expressed and purified in vitro. (A). Expression of the START domain of Dlc2 was confirmed in cell extracts (a) and cell lysates (b) by both the His-tag staining (upper panel) and western blot analysis using monoclonal anti-Histag antibody (bottom panel). (B) Purification of the START domain of Dlc2. (i) Histogram showing the elution of the START domain on an ÄKTA® Purifier™ FPLC system. (ii) SDS-PAGE of the purified His-tagged START domain stained by coomassie blue. Lanes (a) and (b) are molecular mass markers and purified START, respectively.

The START/PET cloning was confirmed by sequencing. Expression of the recombinant His-tagged START domain was confirmed by both His-tag staining and western blotting using an anti-His tag antibody Figure (3A). The recombinant START domain was purified to homogeneity by fast protein liquid chromatography (FPLC) (Figure 3B). Unlike conventional His-tagged protein purification, the purification of the START domain was undertaken at pH 6.4 instead of pH 7.5 to 8.0 to take advantage of the low isoelectric point of the START domain (calculated theoretical pI is 5.9), in order to minimize the nonspecific binding of bacterial proteins, which are usually positively charged at this pH and to minimize the electric attraction of metal ions at acidic pH. The apparent molecular weight for the START domain was 26 kDa as determined by SDS-PAGE, consistent with the calculated molecular weight.

Lipid Bindings of START Domain

To determine whether the START domain directly interacts with various lipids, we performed a protein-lipid overlay assay using the nitrocellulose (Hybond C) membrane [12]. As shown in Figure 4, C16-ceramide and four of its derived lipids S1P, C1P, sphingosine, and AA exhibited strong binding to the START domain. No binding was detected with the ceramide precursor dihydroceramide and one of its derivatives, SM. Moreover, ceramide

exhibited a concentration-dependent binding to the START domain of Dlc2. As a control binding to the negatively charged lipid was investigated. A previous study had shown that phosphatidylinositol 4, 5-bisphosphate (PIP2) can bind to the positively charged polybasic region (PBR) of Dlc1 [13]. This research shows that there is minimal binding of PIP2 to the START domain of Dlc2. This is likely due to lack of a PBR region in the START domain of Dlc2.

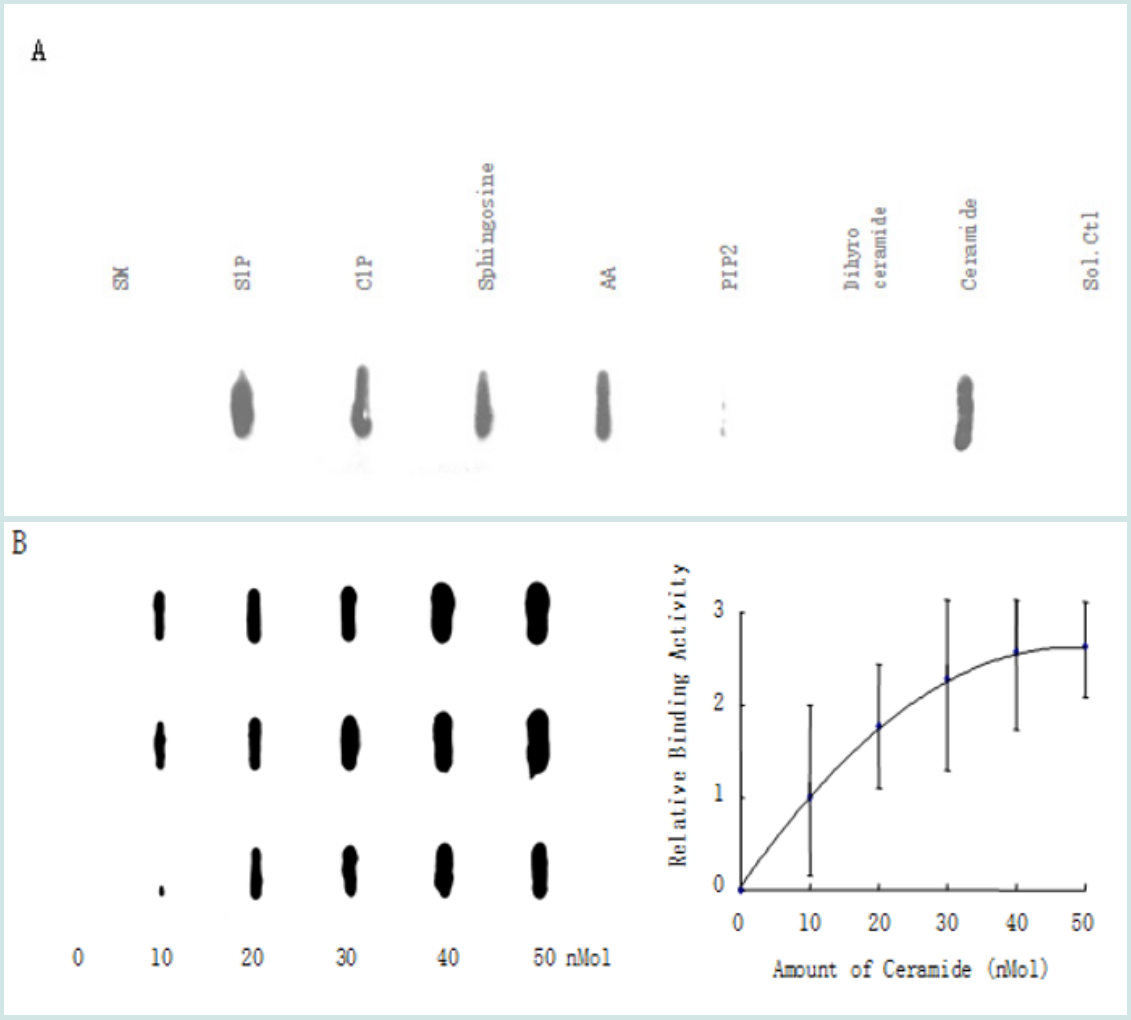

Figure 4: Binding of the START domain to lipids. (A) Protein overlay assays demonstrated the strong binding of the START domain to C16-ceramide, S1P, C1P, sphingosine, AA, and minimal binding to PIP2; while SM and dihydroceramide showed no binding to START. (B) C16-ceramide binding to START in a concentration-dependent manner (n=3).

The binding between ceramide and the START domain of Dlc2 was further confirmed by surface plasmon resonance (SPR) using a Biacore nitrilotriacetic acid (NTA) sensor chip, which is specific for His-tagged proteins. The Biacore chip is able to measure the change of reflection index due to the mass loaded onto the top of the chip in terms of resonance units (RU). His-tagged START was loaded onto the chip and then ceramide or its analog C2-ceramide or dihydroceramide were injected onto the top of the immobilized START domain. The sensorgraph (Figure 5) indicated strong binding between the START domain and ceramide as well as its analog C2 ceramide, which is often used in cell line studies due to its ability of membrane penetration. On the other hand, no binding was observed for the ceramide precursor, dihydroceramide. These data supported specific interaction between the START domain and ceramide. Due to the limitation of NTA chip that is not good for negatively charged group and small analyte, more relative lipids will have to be studied using an alternative chip, the Biacore L1 chip, in future studies.

Ceramide Binding to the STAR Domain Enhances Dlc2 RhoGAP Activity

In order to determine whether the ceramide binding to the START domain has a physiological function, we measured the RhoGAP activity of Dlc2 on Rho recombinant protein using a charcoal precipitation method that can avoid potential errors [14] (Figure 6). Dlc2 RhoGAP protein was cloned and expressed in PET

vector and purified by FPLC following an established protocol [15-17]. As shown in Figure 6, both ceramide and its analog C2- ceramide significantly increased the Dlc2 RhoGAP activity. Although C1P, S1P, sphingosine and AA were able to bind to the START domain of Dlc2 in protein-lipid overlay assay, they did not significantly alter RhoGAP catalytic activity. We confirmed these results using the traditional nitrocellulose method to verify the ceramide action. Both methods demonstrated that ceramide can enhance the Dlc2 RhoGAP activity.

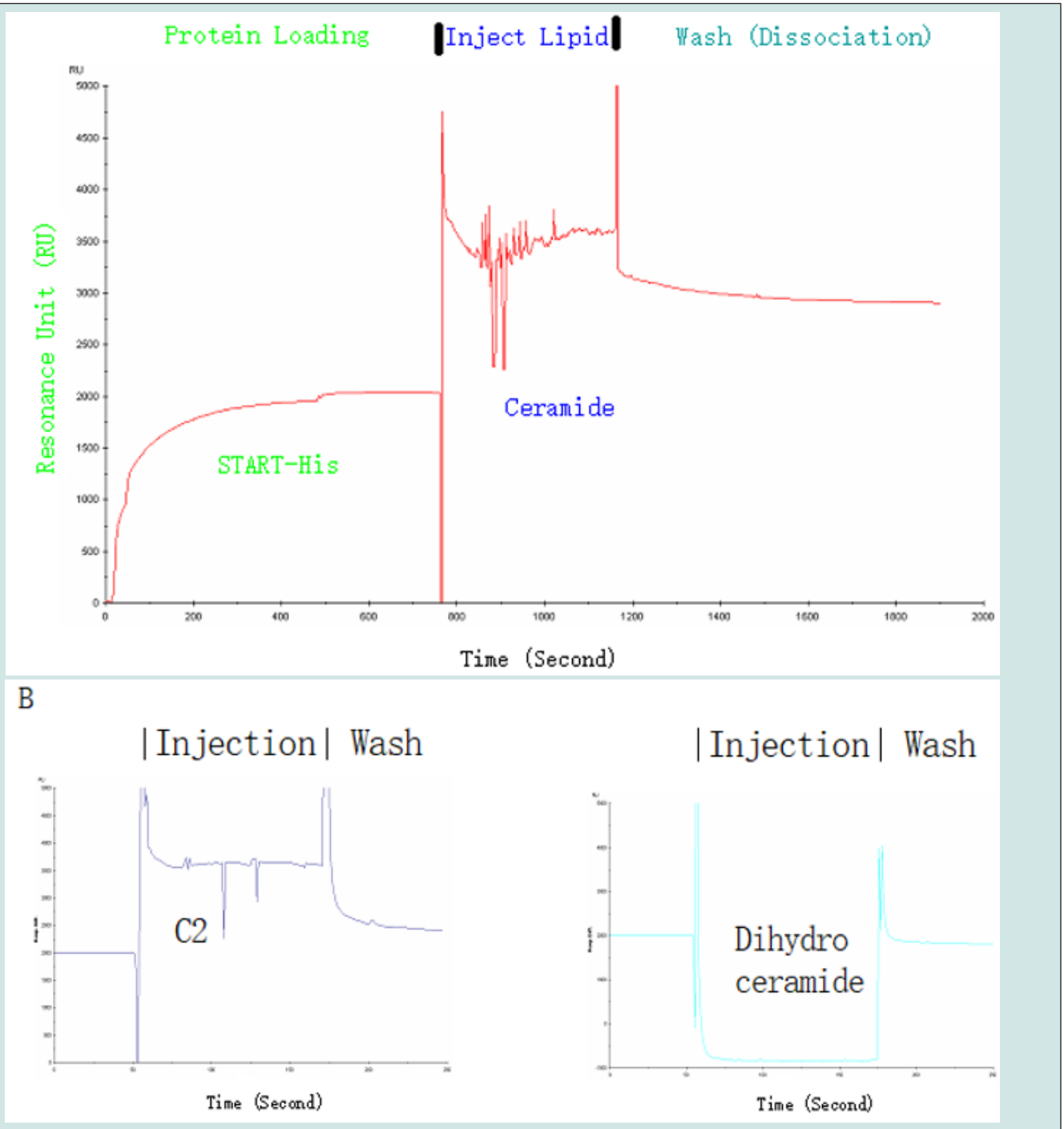

Figure 5: Specific binding of ceramide to the START domain of Dlc2 as demonstrated by SPR. (A) His-tagged protein was loaded to a NTA chip then ceramide was injected onto the top of the START domain and this was followed by washing with running buffer. Elevated resonance indicated the specific binding between the START domain and C16-ceramide. (B) The analog of ceramide, C2 ceramide, exhibited similar binding pattern to the START domain of Dlc2 (left); while no specific binding was detected for dihydroceramide (right).

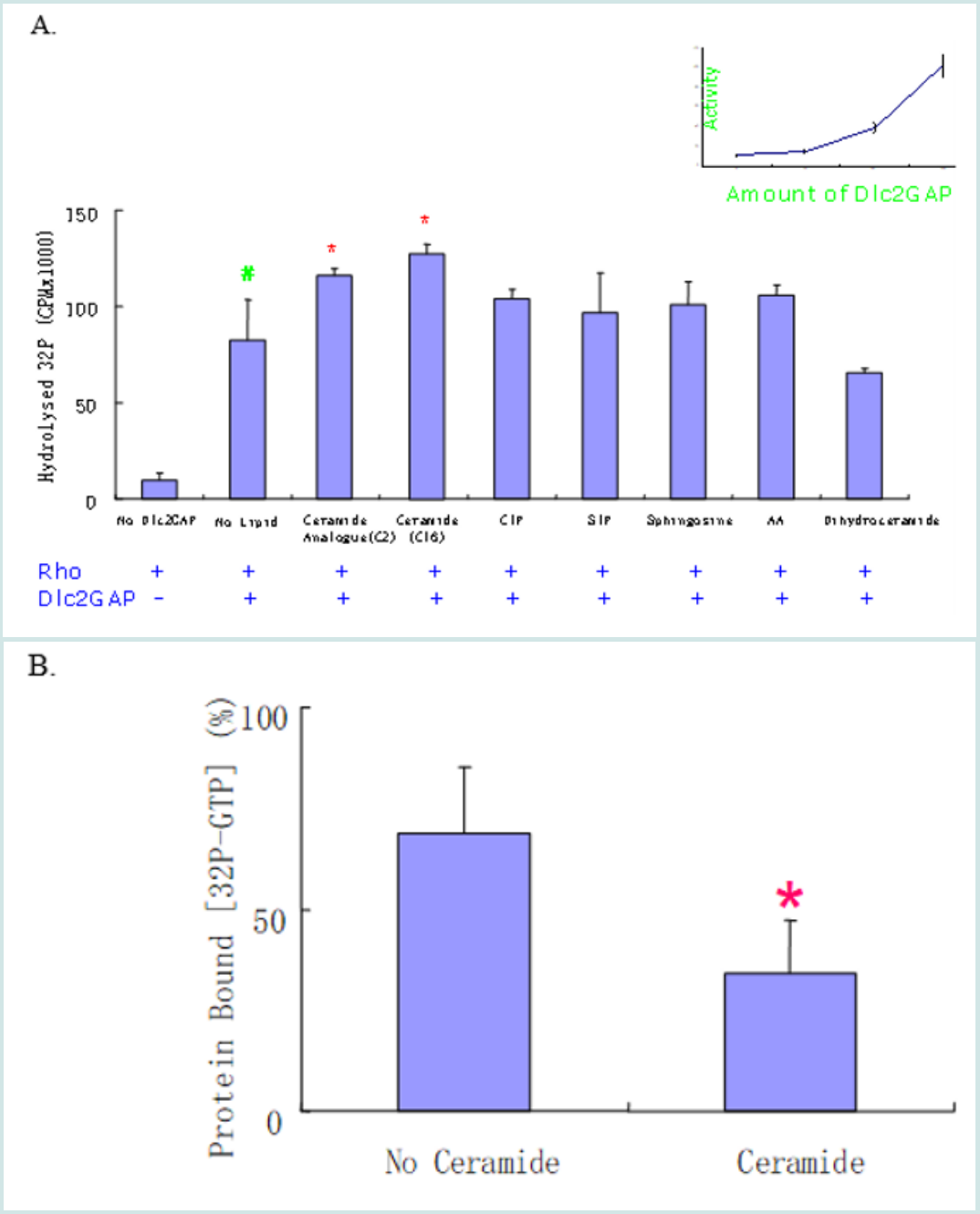

Figure 6: Ceramide enhanced the RhoGAP activity of Dlc2. (A) RhoGap activity was determined in the absence or presence of various lipids using charcoal precipitation method (n=3). "+" refers to the presence of Rho or Dlc2GAP; "-" means absent. Inset: concentration dependent increase of GAP activity with the increase of Dlc2 between 0.3 and 3 nM (n=3). (B) The nitrocellulose filter method confirmed the ceramide positive regulation as well. In the filter method, the values are normalized to the values of preparations without Dlc2, which is assumed as 100% by convention. * $p<0.05$. # $p<0.001$ (n=3).

Ceramide Suppresses Rho Activity in Mitochondria

To investigate whether the enhanced Dlc2 activity induced by ceramide can suppress Rho activity in live cells, active RhoGTPase activity was determined using a Rho biosensor that is able to detect active GTP bound Rho [18]. The biosensor was constructed with a yellow fluorescent protein (YFP) tagged RhoA (the most common type of Rho proteins) at one end and cyan fluorescent protein (CFP) fused to the Rho binding domain (RBD) of rhotekin at the other end. RhoA will only bind to RBD when it is active. The binding between RhoA and RBD will bring YFP and CFP together and provide the energy transfer of florescent resonance. Thus, when excited by CFP

excitation wavelength at 436 nm, the biosensor with inactive Rho will only emit light at the normal wavelength range of CFP [λ=470 nm]; while the biosensor with active Rho will emit light in the wavelength of YFP [λ=535 nm], which is the FRET (Fluorescence Resonance Energy Transfer) signal. The ratio of FRET and CFP has been used previously to determine the level of active Rho level [19]. The target cells were used MMTV NIC cells. This biosensor has been co-localized in mitochondria by living stain using Mitotracker from Life Technologies (Figure 7A). This is in line with the majority of literature that RhoA signaling locates in the mitochondria. Besides the wide type MMTV NIC cells B13 (MMMTV-NIC+/-; Dlc2 +/+), heterozygous C13 (NIC+/-; Dlc2 exon3de/+) cells were also developed to study the effect of ceramide on Rho activity. The Dlc2 expression levels were confirmed by western blot (Figure 7B). With Dlc2 knock-down, the C13 cells show higher Rho signaling than the wildtype B13 cells (Figure 8). Further, this research shows C2 Ceramide significantly reduced active Rho signaling in C13 cells (*p<0.001).

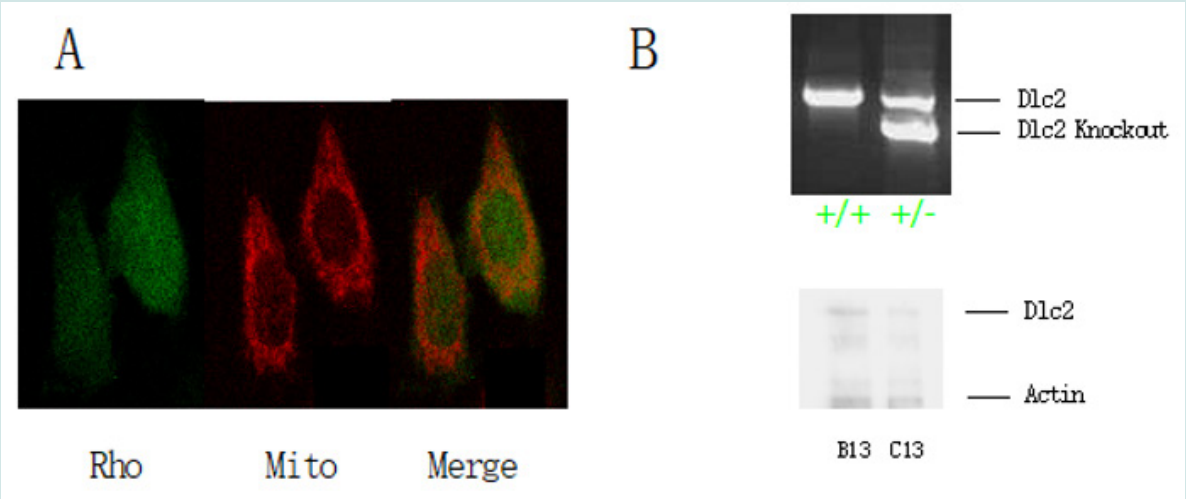

Figure 7: Ceramide signaling in TTMV NIC cells. (A) Active Rho signaling is co-localized in mitochondria. The active Rho was labelled as green while mitotracker, the stains the mitochondria inside a cell, was red. (B) Upper: the Dlc2 exon 3 deletion was confirmed in heterozygous (Dlc2+/-) genome by PCR as compared to wild type (Dlc2+/+). Bottom: western studies showed the underexpression of Dlc2 in C13 (Dlc2+/-) comparing to B13 (Dlc2+/+).

Structural Model of mDlc2 and Predictions of the Ceramide Binding Pocket

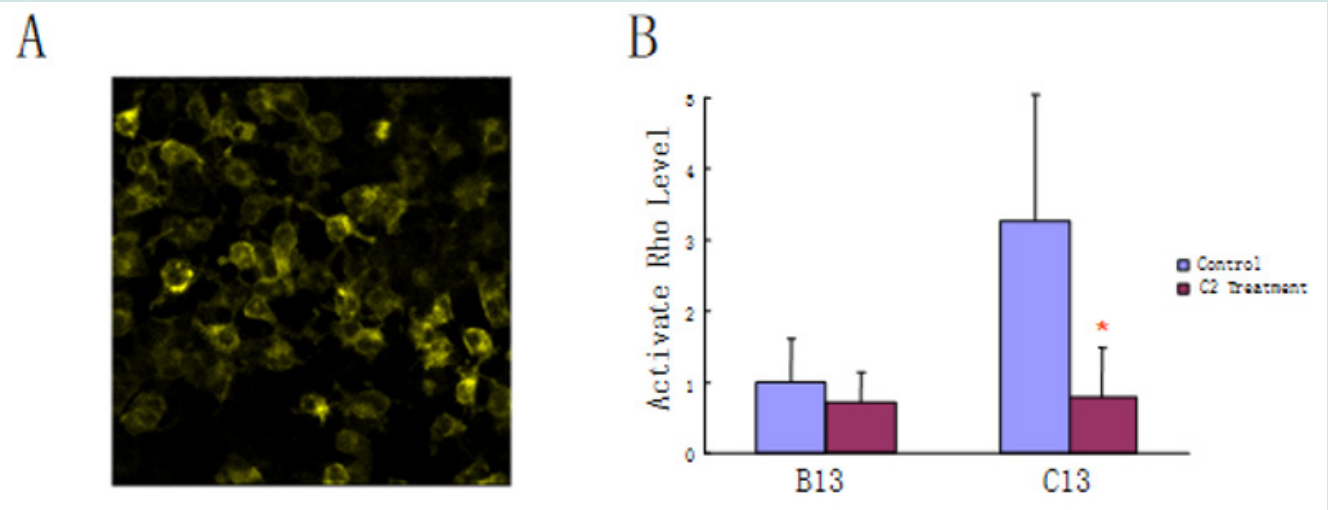

Figure 8: Ceramide inhibited Rho signaling in mitochondria. (A). FRET image. As aforementioned, the exciting light for CFP (cyan fluoresce protein) did not produce cyan color light; instead, via FRET, it produced the emission light in the wavelength of yellow color. (B). Ceramides were able to reduce active Rho signaling slightly in B13 cells and significantly (*p<0.001) in C13 cells.

The biological function of a protein is determined by its three-dimensional structure. Since the abovementioned experiments used mice to produce biological samples, to keep consistent, hereby we will use the mice (m) Dlc2 for modelling. Although the crystal structure of mDlc2 START has yet to be determined, the structure of its human counterpart has been reported (PDB #2PSO) [20]. The human START structure was acquired by X-ray crystallography [19]. During crystallization, there were three asymmetric units per unit cells. Thus, in vitro, the START domain formed a trimmer and each monomer had exactly the same structure. However, the trimmer of Dlc2 START is unlikely to exist in living cells since the START domain only contributes to 18% of the whole Dlc2 molecule and the rest of regions in Dlc2 have strong steric hinderance for START domain monomer interaction. Nevertheless, ceramide best fitted into a putative pocket formed in the junction area of the three START domains (Figure 9).

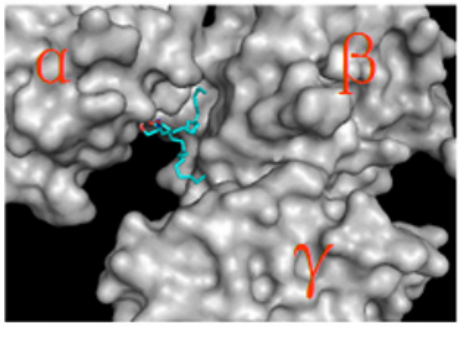

Figure 9: The best-fit ceramide binding site was located on the junction region of the putative trimmer of the human Dlc2 START domain. Ceramide is shown in stick model. Each unit of the putative trimmer was labelled as α, β and γ, respectively.

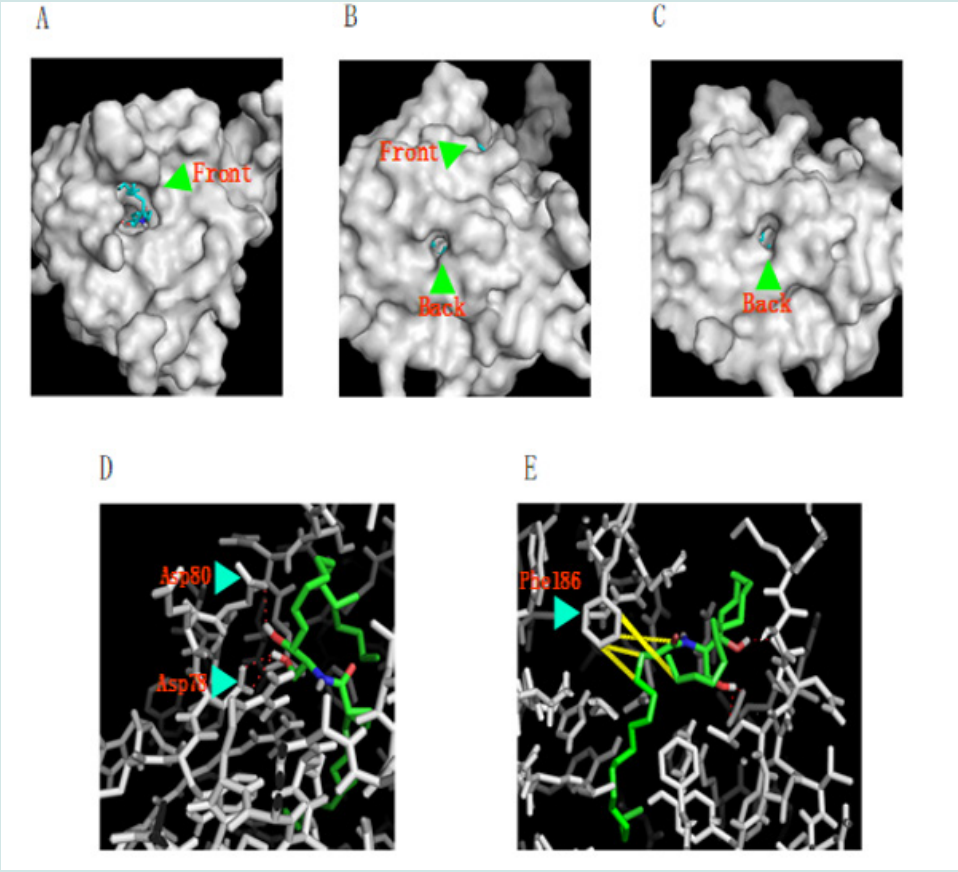

Figure 10: The putative ceramide binding pocket in the START domain. Ceramide is shown in stick model. As a close check, the pocket has a tunnel shape with two open ends. (A), (B) and (C) are, respectively, the front view, the side view (with the ends of the tunnel labelled) and the back view of the ceramide binding pocket. (D). The hydrogen bond interactions between ceramide and Asp78/80 are shown as red dotted lines. (E). The π interactions are show as yellow dashed line. The depth of field was adjusted in (D) and (E) to set the interacting residues onto the in-focus planes for clear viewing.

Since there are 95% sequence identify between human and mDlc2 START domains, the structural modelling of mDlc2 START was applicable and should be helpful in identifying the lipid binding pocket and elucidating the biological function of START. We thus built a structural model of mDlc2 START domain by computer modeling using SWISS-MODEL server [21-22]. To study the detailed structure of a single START domain. Ceramide was able to dock in the mDlc2 START domain in the model. The active site situated in a deep pit on the surface. The hydrophobic residues surrounding the pit, Leu39, Ala40, Phe41, Ala55, Phe81, Val82, Val100, Leu101, Leu132, Val145, Ile169, Ile172, Leu174, Phe186, Leu189, Ala191, Ala192, Val194, and Ile197, provide hydrophobic interactions with ceramide. There are also several polar residues around the pockets. As well there are a few positively charged basic residues (e.g. Lys92, Arg110, and Lys175) that might be able to interact with lipids with negatively charged groups such as S1P, C1P and AA. PIP2, which is twice as large as ceramide, was hard to fit into the pit. As a close examination on the binding site, a hollow tunnel was identified (Figure 10A-C). This unique shape might play a role in the lipid transporting actions of the STARD protein family. The oxygen atoms in the side-chain of Asp78 and Asp80 could interact with hydrogen atoms in the –OH groups in the sphingosine part of ceramide and aid in orienting the ceramide molecule in its binding pocket (Figure 10D). π noncovalent interactions between the aromatic ring of Phe186 and the approximal side of the fatty acid chain as well as the side chain of the sphingosine part in ceramide are identified (Figure 10E). The sphingosine in ceramide would exhibit a good interaction with the binding pocket as sphingosine is a small molecule that is easy to enter the pit. Therefore, it is not surprising that sphingosine was able to bind to START in the overlay assay.

We suspected that the START domain of Dlc2 might undergo significant conformational change, such as domain movements, to affect the conformation of the nearby RhoGAP domain to apply allosteric regulation during the GAP catalysis. According to our RhoGAP activity data, we suggest that the binding with ceramide lipid might be explained by the key and lock theory. Only the right configuration and size of the ligand can trigger significant and appropriate conformation changes that are required for RhoGAP activity regulation. Further ceramide STARD13 cocrystallization X-ray studies will be required to determine the catalytic mechanism of Dlc2.

Discussion and Conclusion

In the current study, we demonstrated its interaction with ceramide and Dlc2 plays a positive role to inhibit the tumorigenic Rho signalling, via stimulating Dlc2 GAP (also called the RhoGAP of Dlc2) activity that inactivates the Rho. Moreover, this research demonstrates that the ceramide is able to bind to START domain of Dlc2 and allosterically enhance its RhoGAP activity. This will subsequently inactivate Rho and suppress cancer. In fact, the Dlc2-related therapeutic molecular design is more likely to be achieved because the Dlc2 pathway is relatively simply comparing with other multiple-pathway tumor suppressors, like RIZ1 [23], which interact with downstream tumor suppressors that also have their own pathways that involved other molecules [22], which subsequently have their own pathways. And so on……. It could enter infinite cycles.

In order to develop the personalized medicine that precisely treats cancer patients with the Dlc2 deficiency, we proposed a two-step plan, which could lead to a well-designed therapy that is highly specific with minimal negative effects. In the first step, we design a recombination protein that expresses the sequence of Dlc2. This recombination protein will serve as a biotherapeutic that will be administrated into patients. This will help patients to overcome the deficiency of Dl2 and may show better response to general cancer drugs. As a matter of fact, tens of macromolecular drugs have been made successful due to the recent progress in drug deliver. Artificial Intelligence (AI) has been applied to the design of medicinal macromolecules, such as designing antimicrobial peptides (AMPs). However, current AI is limited; but the future would be bright if the AI could be performed by a quantum computer, since the calculations that used to take a modern high-end computer thousands of years can be easily achieved by a quantum computer in tens of seconds [24]. In the second step, a ceramide drug will be designed to serve as an enhancer. It is worthy of mentioning that it is very rare to only use natural ceramide as a drug, because it can be easily digested by a number of enzymes in human body. Thus, the ideal drug molecule will be a chemical molecule with the ceramide molecular structure as the main structure whiling adding a chemical group to avoid to be digested. The designed molecule is expected to have better bioavailability and longer half-life period inside human body. The ceramide drug will fight against cancer through the above-mentioned pathway.

Hereby, we named the above-mentioned two-step drug design as the Sun Strategy in Drug Development, which is theoretically one of best approaches for developing precision medicine to treat patients with special gene deficiency. The strategy combined both the emerging macromolecular drug design and the classic small molecular design: first of all, a biotherapeutic molecule will be developed to compensate the gene deficiency; second, rational drug design will be performed to enhance the function of the biotherapeutic molecule in vivo. This combination is expected to significantly reduce the side effects as observed in many biotherapeutics. After all, there are concerns of potential side effects while using recombination protein as a drug. The use of an enhancer, e.g. a secondary small molecule, will improve the action of the therapeutic protein drug and keep the administrated dose of a protein drug to the minimal level. This will dramatically reduce the side effects while easing the difficulties encountered during the macromolecular drug deliveries.

All in all, the interaction of ceramide and Dlc2 is well studied, and such interaction has provided value clues for innovative drug discoveries.

Materials and Methods

Cloning and Expression of the Gene Fragment Encoding the START Domain

A plasmid containing the full-length Dlc2 gene was kindly provided by Dr. Sabbir of the Manitoba Institute of Cell Biology. Using the plasmid DNA as the template and a pair of DNA primers (forward: 5'-CATATGCTGGAAGACTTGGGAG-3' with a NdeI restriction site; backward: 5'-CTCGAGTTTTGTTTCTGGACCCT-3' with a XhoI restriction site) with their sequences corresponding to the 5' and 3' ends of the gene fragment encoding the START domain of Dlc2 respectively. The PCR product was cleaned using a QIAquick PCR purification kit (Qiagen, Toronto, Ontario, Canada) and then digested with restriction endonucleases NdeI and XhoI. The digested DNA fragment was cloned into the expression vector pET28a(+) (Merk Millipore, City, State?) at the NdeI and XhoI sites. The resulting plasmid pET28/START was transformed into E. coli DH5 α cells. Plasmid DNA was extracted from positive clones on Luria-Bertani (LB)-agar plates containing kanamycin (25mg/ml), and verified by sequencing at Cancer Care Manitoba (Winnipeg, Manitoba, Canada). Then the plasmid was transformed into E. coli BL21(DE3) pLysS cells for over-expression of the START domain. One liter of LB plus kanamycin medium was inoculated with 5.0 mL of overnight culture from a single colony of transformed E. coli BL21(DE3) pLysS cells and incubated at 37 °C with shaking at 250 rpm until OD600 of the culture reached 0.6. Protein expression was induced by adding IPTG (final concentration of 1 mM) to the cell culture. Cell growth was allowed to proceed for an additional 4 hours. The cells were harvested by centrifugation at 5,000 g for 20 minutes and the pellets were stored at -80 °C.

Western Blot and Histidine-Tag Staining

To detect the expression of His-tagged START, Western Blot was performed by the standard technique as previous reported [24]. The primary antibody is a monoclonal His-tag antibody from Sigma-Aldrich (St. Louis, Missouri, USA). The His-tag stain was performed using a His-tag stain kit (Thermo Fisher, Toronto, Ontario, Canada) and visualize in a UV transluminitor (Syngene, Frederick, Maryland, USA). The BL21(DE3) pLysS cells that expressed START were lysed in BugBuster reagent (EMD Milipore Chemicals, Gibbstown, New Jersey, USA), and raw extract of the START protein was prepared as previous reported [25].

Purification of the START domain

START domain is purified to homogeneous by affinity chromatography an ÄKTA® Purifier™ FPLC system from General Electric (GE; Toronto, Ontario, Canada). A frozen pellet from 1 L cell culture was suspended in 40 mL of the lysis buffer (20 mM Tris-HCl, pH 6.4, 0.3 M NaCl, 10 mM imidazole, 0.5 mM phenylmethylsulphonyl fluoride (PMSF), 5 mM β-mercaptoethanol (β -ME), 1 μM pepstatin A, and 1 g/L lysozyme) and incubated with gentle rotation for 30 min. The cells were further disrupted by sonication using a Sonifier™ 350 sonicator from Branson Ultrasonics (Danbury, Connecticut, USA). The cell lysate was centrifuged at 20,000 g for 30 min. The supernatant was loaded two series-connected 1-mL HisTrap FF columns (GE) pre-loaded with Zinc ions. The column was washed thoroughly with about 50 mL of the wash buffer (buffer A; 20 mM Tris-HCl, pH 6.4, 0.3 M NaCl, 50 mM imidazole, 0.5 mM PMSF, 5 mM β -ME, and 1 μM pepstatin A) at a flow rate of 2 mL/min until the elute UV absorbance was approximately zero. The START domain was then eluted with gradient wash using the elution buffer (buffer B; 20 mM Tris-HCl, pH 6.4, 0.3 M NaCl, 100 mM imidazole, 0.5 mM PMSF, 5 mM β -ME, and 1 μM pepstatin A). Purity of the START domain was examined by SDS-PAGE.

Protein-Lipid Overlay Assay

The protein-lipid overlay assay is adapted from a published method [12]. Briefly, the lipids (SM, C1P, S1P, sphingosine, AA, PIP2, ceramide, and dihydroceramide) were purchased from Avanti Polar Lipids (Alabaster, Alabama, USA). They were spotted onto Hybond C membrane (GE), which was pre-wet in phosphate buffer system (PBS), through a slot blotter (Sigma-Aldrich) under vacuum. The membrane was blocked for 1 h in 3% fatty acid-free bovine serum albumin (FAF-BSA) in PBST (0.1% Tween 20 in PBS). Then, the membrane was hybridized with 0.2 μg/ml the His-tagged START in 3% FAF-BSA/PBST 2 hour at room temperature. The membrane was rinsed six times for 5 min with PBST and then exposed to a 1:5000 dilution of His-tagged monoclonal antibody mouse IgG (Sigma-Aldrich) in 3% FAF-BSA/PBST for 1 h at room temperature. After that, the membrane was washed six times for 5 min with PBST and then exposed to a 1:2500 dilution of anti-mouse IgG-horseradish peroxidase (Santa Cruz Biotechnology, Santa Cruz, California, USA) in 3% FAF-BSA/PBST for 1 h at room temperature. The membrane was then washed 6 times for 5 min with PBST and 1 time for 5 min with PBS before developed by the enhanced chemiluminescence (ECL) kit from GE. At least three repetitions were performed for each assay. Biorad Quantity One software was executed for density quantification.

SPR Resonance

The binding between START and ceramide was further investigated by SPR, that was performed using a Biacore 2000 instrument (GE) operating at 25ºC. The running buffer used in all experiments was 50 mM PBS with 0.005% NP40, pH7. All experiments were performed on a NTA coupled sensor chip (GE). Immobilization of the His-tagged START was done using the protocol supplied with the sensor chip. Briefly, two flow cells on the NTA-sensor chip were activated by a 1 min injection of NiCl2 (500 μM) at 20 μL min-1. The his-tagged START protein was immobilized onto one of the flow cells. The other flow cell served as a reference surface to subtract any non-specific binding that may occur. Binding activity between START and the ceramide was tested by injecting the ceramide or its analog C2 or its precursor solution at a rate of 20 μL min-1, followed by dissociation with running buffer. Each experiment was performed in duplication and achieved same binding patterns.

RhoGap Assay

The activity of the Dlc2 RhoGAP was assayed by 32P-labelled GTP hydrolysis. Both charcoal precipitation and nitrocellulose filter methods were performed according to previous report [14]. Dlc2 and Rho were prepared from bacteria expression systems. His-tagged Dlc2 expressed by PET28a(+) vector is purified according to a previous protocol [27]. The Rho was expressed from pGEX-2T/RhoA plasmid [17] and purified by affinity chromatography. The column is packed by glutathione Sepharose 4B beads (GE). The buffer formulas followed the previous report [28]. The radioactivity was measured using a scintillation spectrometer (Beckman Coulter, Toronto, Ontario, Canada). The lipids were dissolved in warmed ethanol with sonification in a Sonifier™ 350 sonicator from Branson Ultrasonics and then diluted into 0.1mg/ml (same concentration as in the previous RIA report [14] in 10% ethanol. In no lipid controls, the lipid solutions were replaced with 10% ethanol.

Developing MMTV NIC cell lines

Three lines of mice were used 1) The Dlc2 (Stard13tm1a(KOMP) Wtsi) conditional (floxed) knock-out mice were obtained from the NIH Knock-Out Mouse Project (KOMP) Repository at University of California Davis (www.komp.org). The flanking βgeo cassette was removed by crossing to the Flp recombinase expressing mice (B6.Cg-Tg(ACTFLPe)9205Dym/J, Jackson Laboratory, Bar Harbor, ME) resulting in Dlc2 exon3flox/+ mice. 2) The mammary tumor generating mice MMTV (mouse mammary tumor virus)-NIC (containing activated Neu (ErbB2) oncogene and Cre recombinase expressed from the same bicistronic transcript under control of MMTV promoter) were obtained from Dr. Bill Muller, McGill University. 3) These mice have been interbred to obtain the heterozygous and homozygous Dlc2 exon3 deleted mice with the MMTV-NIC oncogene. Cell lines from tumors of 1) MMTV-NIC (Dlc2+/+), 2) MMTV-NIC and 3) Dlc2 exon3flox/+ and MMTV-NIC, Dlc2 exon3flox/flox mice were established as described below. The genotypes of mice and tumors were verified by PCR.

The mammary tumors were isolated and washed by PBS to remove debris and blood cells. The tumors were minced and digested with 2 mg/ml collagenase and 0.8mg/ml dispase in Dulbecco's Modified Eagle Medium (DMEM) at 37°C for 2 hours. The cellular suspension was centrifuged at 500 g for 10 min. The cell pellets were resuspended in DMEM containing 2% fetal bovine serum (FBS) and a set of growth factors (1 μg/ml hydrocortisone, 5 μg/ml insulin, 5 ng/ml epidermal growth factor and 35 μg/ml bovine pituitary extract) for overnight at 37°C in 5% CO2. Unattached cells and debris were removed, and fresh medium was added to the adherent cells. Then the cells were loaded to matrigel (Collaborative Research, Bedford, Massachusetts, USA) for 3D culture. After 1-week, single colonies of cells were isolated to culture. MMTV NIC cell lines B13 were developed from Dlc2 exon3+/+ serving as a wild type control.

The mice used in this study were treated with humane care in compliance with the Canadian Council on Animal Care Guide. The experimental protocols have been approved by the by University of Manitoba.

Biosensor Study

The Rho biosensor able to sensor the active RhoGTPase by FRET was ordered from AddGene (Cambridge, Massachusetts, USA; Plasmid 12602: pBabe-Puro-RhoA Biosensor). The biosensor contains defective pBabe retrovirus and is constructed with CFP and YFP, and the ratio of FRET and CFP is used as a way to measure the active Rho level. The pBabe retrovirus vector needs a packing cell line to produce a full potential virus. The vector is successfully transfected into Pheonix-Eco cells by the calcium phosphate precipitation method. The Pheonix-Eco cell line is a helper-free packaging cell line to produce infective retrovirus, which then introduce and overexpress the biosensor into the target cells, B13 and C13 cells. The expressions of the Rho biosensor were confirmed by fluorescent live cell microscopy as reported [18]. After transfection with the biosensor, the B13 and C13 cells were treated with 30 μM C2-ceramide for 24 hours. Then, mitochondria fractions of B13 and C13 cells were isolated as reported [29]. The mitochondria preparations were resuspended in the Raichu buffer [30] and put into the fluorescence reading plates (Corning, Tewksbury, Massachusetts, USA). To quantify the active Rho level, the fluorescence was read in a SpectraMax GeminiXS machine (Molecular Devices, Sunnyvale, CA, USA). The excitation wavelength is 433 nm, and the emission ratio of YFP (FRET at 530 nm) and CFP (at 475 nm) fluorescence was calculated. Data were normalized to the basal active Rho level in B13 mitochondria fractions.

In silico simulations

To study the interaction between ceramide and START domain, the mDlc2 START model was generated by SWISS-MODEL. The geometry and energy criteria for the model were evaluated by PROCHECK, WHAT IF and Verify3D. Ceramide was docked into the active site of the START domain using AutoDock Vina [31]. To study the binding pocket of CERT START, ArgusLab docking software was applied to dock S1P into the ceramide binding pocket of the CERT START, due to its exceptional ability of examine whether a ligand can bind to a define pocket. To generate pictures highlighting the hydrogen bonds and pi interactions, the depth of fields were adjusted by PyMol (DeLano Scientific LLC, Palo Alto, California, USA) in an Ubuntu Linux System (London, UK) for the best view on relevant residues.

Acknowledgements

Acknowledge to the animals who scarify themselves for the scientific research. It is noteworthy that not all of the authors agree that human are evolved from animals. Indeed, one of the authors have proposed the Sun Theory of Evolution, promoting the idea that the human is not evolved from animals. If not from animals, where are humans originally from? Well, we could from parallel civilizations [32] in the universe; anyway, human beings are not evolved from monkeys. Hope these ideas will reduce the usage of animals who are scarified for science.

References

1. Xue W, Krasnitz A, Lucito R, Sordella R, Vanaelst L, et al. (2008) DLC1 is a chromosome 8p tumor suppressor whose loss promotes hepatocellular carcinoma. Genes Dev 22(11): 1439-1444.
2. Durkin ME, Ullmannova V, Guan M, Popescu NC (2007) Deleted in liver cancer 3 (DLC-3), a novel Rho GTPase-activating protein, is downregulated in cancer and inhibits tumor cell growth. Oncogene 26(31): 4580-4589.
3. Sun W and Yang J (2010) Functional mechanisms for human tumor suppressors. J Cancer 1: 136-140.
4. Ullmannova V and Popescu NC (2006) Expression profile of the tumor suppressor genes DLC-1 and DLC-2 in solid tumors. Int J Oncol 29(5): 1127-1132.
5. Kim TY, Vigil D, Der CJ, Juliano RL (2009) Role of DLC-1, a tumor suppressor protein with RhoGAP activity, in regulation of the cytoskeleton and cell motility. Cancer Metastasis Rev 28(1-2): 77-83.
6. Popescu NC and Goodison S (2014) Deleted in liver cancer-1 (DLC1): an emerging metastasis suppressor gene. Mol Diagn Ther 18(3): 293-302.
7. Frame MC, Brunton VG (2002) Advances in Rho-dependent actin regulation and oncogenic transformation. Curr Opin Genet Dev 12(1): 36-43.
8. Jaffe AB, Hall A (2002) Rho GTPases in transformation and metastasis. Adv Cancer Res 84: 57-80.
9. Krijnen PA, Sipkens JA, Molling JW, Rauwerda JA, Stehouwer CD, et al. (2010) Inhibition of Rho-ROCK signaling induces apoptotic and non-apoptotic PS exposure in cardiomyocytes via inhibition of flippase. J Mol Cell Cardiol 49(5): 781-790.
10. Kudo N, Kumagai K, Tomishige N, Yamaji T, Wakatsuki S, et al. (2008) Structural basis for specific lipid recognition by CERT responsible for nonvesicular trafficking of ceramide. Proc Natl Acad Sci U S A 105(2): 488-493.
11. Sun W, Leslie H, Xu F Y, Wilkins J A, Dustin L, et al. (2012) The Interaction between Ceramide and the Deleted in Liver Cancer 2. Paper presented at the Frontiers in Lipid Biology, The American Society for Biochemistry and Molecular Biology (ASBMB). International Conference on the Bioscience of Lipids (ICBL). Canadian Lipoprotein Conference (CLC). Banff, Canada.
12. Pettus B J, Bielawska A, Subramanian P, Wijesinghe D S, Maceyka M, et al. (2004) Ceramide 1-Phosphate Is a Direct Activator of Cytosolic Phospholipase A2. Journal of Biological Chemistry 279(12): 11320-11326.
13. Erlmann P, Schmid S, Horenkamp F A, Geyer M, Pomorski T G, et al. (2009) DLC1 activation requires lipid interaction through a polybasic region preceding the RhoGAP domain. Mol Biol Cell 20(20): 4400-4411.
14. Ligeti E and Settleman J (2006) Regulation of RhoGAP specificity by phospholipids and prenylation. Methods Enzymol 406(1): 104-117.
15. Sun W, Geyer C R, Yang J (2008) Cloning, expression, purification and crystallization of the PR domain of human retinoblastoma protein-binding zinc finger protein 1 (RIZ1). Int J Mol Sci 9(6): 943-950.
16. Sun W, Qiao L, Liu Q, Chen L, Ling B, et al. (2011) Anticancer activity of the PR domain of tumor suppressor RIZ1. Int J Med Sci 8(2): 161-167.
17. Sun W, Sammynaiken R, Chen L, Maley J, Schatte G, Zhou Y, et al. (2011) Sphingobium chlorophenolicum dichlorohydroquinone dioxygenase (PcpA) is alkaline resistant and thermally stable. Int J Biol Sci 7(8): 1171-1179.
18. Pertz O, Hodgson L, Klemke R L, Hahn K M (2006) Spatiotemporal dynamics of RhoA activity in migrating cells. Nature 440(7087): 1069-1072.
19. Holeiter G, Heering J, Erlmann P, Schmid S, Jahne R, et al. (2008) Deleted in liver cancer 1 controls cell migration through a Dia1-dependent signaling pathway. Cancer Res 68(21): 8743-8751.
20. Thorsell A G, Lee W H, Persson C, Siponen M I, Nilsson M, et al. (2011) Comparative structural analysis of lipid binding START domains. PLoS One 6(6): 19521.
21. Arnold K, Bordoli L, Kopp J, Schwede T (2006) The SWISS-MODEL workspace: a web-based environment for protein structure homology modelling. Bioinformatics 22(2): 195-201.
22. Kiefer F, Arnold K, Kunzli M, Bordoli L, Schwede T (2009) The SWISS-MODEL Repository and associated resources. Nucleic Acids Res 37(1): 387-392.
23. Sun W and Yang J (2014) Tumor Suppressor RIZ1 in Carcinogenesis. Journal of Carcinogenesis & Mutagenesis 5(2): 160.
24. Sun W (2024) Solving the Darwinian Paradoxes by "Sun Model of Civilization", Re-Examine the Origin of Human. Journal of Anthropological and Archaeological Sciences 9(2): 1200-1211.
25. Hatch G M, Gu Y, Xu F Y, Cizeau J, Neumann S, et al. (2008) StARD13(Dlc-2) RhoGap mediates ceramide activation of phosphatidylglycerolphosphate synthase and drug response in Chinese hamster ovary cells. Mol Biol Cell, 19(3): 1083-1092.
26. Shields C (2010) The role of Dlc-2 in ceramide signaling to PGP synthase. Unpublished M.Sc., University of Manitoba, Winnipeg, Canada.
27. Sun W (2013) Biochemical Analyses of RIZ1 Methyltransferase (PR) and Dichlorohydroquinone Dioxygenase (PcpA). Library and Archives Canada. ISBN-13: 9780494920664, ISBN-10: 0494920661.
28. Einarson M B, Pugacheva E N, Orlinick J R (2007) Preparation of GST Fusion Proteins. CSH Protoc, 2007, pdb prot 4738.
29. Frezza C, Cipolat S, Scorrano L (2007) Organelle isolation: functional mitochondria from mouse liver, muscle and cultured fibroblasts. Nat Protoc 2(2): 287-295.
30. Holeiter, G. (2009). The role of the deleted in liver cancer protein family in breast epithelial cell transformation. Unpublished Ph.D. thesis, Universitat Stuttgart.
31. Trott O, Olson A J (2010) AutoDock Vina: improving the speed and accuracy of docking with a new scoring function, efficient optimization, and multithreading. J Comput Chem 31(2): 455-461.
32. Sun W (2024) Solving the Olbers's Paradox, Explaining the "Red-Shift", and Challenging the Relativities by "Sun Matters Theory" and "Sun Model of Universe", an Evolution of the Einstein's Static Universe Model. Natural Science 16(2): 7-18.

Submission Link: Submit Article

DOI: 10.32474/DDIPIJ.2024.04.000186